

# Farrerol Alleviates Hypoxic-Ischemic Encephalopathy by Inhibiting Ferroptosis in Neonatal Rats via the Nrf2 Pathway

Yongfu LI<sup>1</sup>, Ting WANG<sup>2</sup>, Ping SUN<sup>1</sup>, Wei ZHU<sup>3</sup>, Yirong CHEN<sup>4</sup>, Mo CHEN<sup>5</sup>, Xu YANG<sup>1</sup>, Xiaodong DU<sup>2</sup>, Yuan ZHAO<sup>6</sup>

<sup>1</sup>Department of Science and education, Pu'er People's Hospital, Yunnan, People's Republic of China, <sup>2</sup>Department of Reproductive Medicine, Pu'er People's Hospital, Yunnan, People's Republic of China, <sup>3</sup>Department of Science and education, The People's Hospital of Xishuangbanna Dai Autonomous Prefecture, Yunnan, People's Republic of China, <sup>4</sup>Department of nosocomial infection administration, Pu'er People's Hospital, Yunnan, People's Republic of China, <sup>5</sup>Department of Gastrointestinal and Burn Plastic Surgery, Pu'er People's Hospital, Yunnan, People's Republic of China, <sup>6</sup>Department of Oncology, Pu'er People's Hospital, Yunnan, People's Republic of China.

Received November 16, 2022

Accepted April 18, 2023

## Summary

Farrerol (FA) is a traditional Chinese herbal medicine known for its anti-inflammatory and anti-oxidative properties in various diseases. Ferroptosis is an iron-dependent oxidative stress-induced cell death. It is characterized by lipid peroxidation and glutathione depletion and is involved in neuronal injury. However, the role of FA in inhibiting ferroptosis in hypoxic-ischemic encephalopathy (HIE) and its underlying mechanisms are not yet completely elucidated. This study aimed to investigate whether FA could mediate ferroptosis and explore its function and molecular mechanism in HIE. A neonatal rat model of HIE was used, and rats were treated with FA, ML385 (a specific inhibitor of nuclear factor erythroid 2-related factor 2 [Nrf2]), or a combination of both. Neurological deficits, infarction volume, brain water content, pathological changes, and iron ion accumulation in the brain tissues were measured using the Zea-Longa scoring system and triphenyl tetrazolium chloride (TTC), hematoxylin-eosin (HE), and Perls' staining. The expression levels of GSH-Px, MDA, SOD, and ROS in brain tissues were also evaluated. Western blot analysis was performed to analyze the expression of the Nrf2 pathway and ferroptosis-related proteins. The results showed that FA administration significantly reduced neuronal damage, infarct volume, cerebral edema, and iron ion accumulation and inhibited MDA and ROS levels while promoting GSH-Px and SOD levels. FA also increased the expression levels of glutathione peroxidase 4 (GPX4), solute carrier family 7 member 11 (SLC7A11), Nrf2, and HO-1.

Moreover, the combination of ML385 and FA in HIE abolished the FA protective effects. Therefore, the study concludes that FA exerts a neuroprotective effect after HIE by inhibiting oxidative stress and ferroptosis via the Nrf2 signaling pathway.

## Key words

Farrerol • Hypoxic-ischemic encephalopathy • Ferroptosis • Nrf2 signaling pathway

## Corresponding author

Yuan Zhao, Department of Oncology, Pu'er People's Hospital, NO.44 Zhenxing Road, Simao District, Pu'er 665000, Yunnan, People's Republic of China. E-mail: duguxiaoting@163.com

## Introduction

Neonatal hypoxic-ischemic encephalopathy (HIE) is a leading cause of neonatal death and long-term disability, including visual impairment, learning impairment, epilepsy, mental retardation, blindness, and cerebral palsy [1]. Lack of oxygen is a major contributing factor to brain damage during the neonatal period [2], causing about 1 million deaths per year and being one of the most common causes of neonatal morbidity and mortality worldwide. According to a previous report, about 20 % of all neonates with HIE will die in the newborn period, and 25 % of the survivors will suffer

a permanent neurologic deficit [3]. Despite extensive research efforts, the prevention and treatment of this disease remain a significant medical challenge with global financial repercussions. Therefore, there is an urgent need to study the pathological mechanisms underlying this disease. Currently, oxidative stress is widely accepted as the most crucial pathophysiological mechanism of HIE. Therefore, preventing oxidative stress is considered an effective therapeutic approach for HIE [4]. Recent studies have also shown the involvement of ferroptosis in HIE [5-7]. However, the detailed molecular mechanisms in HIE are not fully elucidated.

Ferroptosis, a form of cell death distinct from apoptosis, necrosis, autophagy, and pyroptosis, is characterized by iron-dependent lipid peroxidation and is involved in aging, immunity, and cancer [8-10]. Oxidative stress inhibits cystine uptake through the glutamate/cystine transporter (also called system xc-) and down-regulates expression of genes such as glutathione peroxidase 4 (GPX4) and solute carrier family 7 member 11 (SLC7A11), contributing to ferroptosis [11]. The nuclear factor erythroid 2-related factor 2 (Nrf2) signaling can counteract oxidative stress and inhibit ferroptosis in lung injury [12, 13]. HIE promotes iron accumulation in the central nervous system, resulting in a series of free radical reactions that lead to nerve cell damage and irreversible brain damage. A recent study demonstrated that ferroptosis is involved in HIE in neonatal rats [7]. Moreover, a natural glycosyl triterpenoid product has been reported to alleviate brain damage related to ferroptosis *in vivo* and *in vitro* [6]. Therefore, we aimed to investigate whether other natural products could protect against HIE by inhibiting ferroptosis.

Farrerol (FA), (S)-2,3-dihydro-5,7-dihydroxy-2-(4-hydroxyphenyl)-6,8-dimethyl-4-benzopyrone, a natural flavanone compound isolated from *Rhododendron* [14], a traditional Chinese herbal medicine, has been reported to exhibit protective effects against bacteria, inflammation, angiogenesis, and oxidative stress-related diseases [15, 16], such as chronic kidney disease [17], myocardial ischemia/reperfusion [18], and hepatotoxicity [19]. A previous study has shown that FA possesses neuroprotective activity in  $\beta$ -amyloid induced oxidative stress through the Nrf2/Keap1 pathway [20]. In another study, FA was found to protect dopaminergic neurons in lipopolysaccharide (LPS)-induced Parkinson's disease (PD) via AKT and NF- $\kappa$ B signaling pathways [21].

Similarly, in a cell model of 1-methyl-4-phenylpyridinium (MPP<sup>+</sup>)-induced PD micro-glia inflammation, FA was found to inhibit the TLR4 signaling pathway and reduce cell inflammation response [22]. These findings revealed that FA played a critical role in neuron protection. However, its role in the HIE model has not yet been explored.

In the present study, we aimed to investigate the protective effects of FA in an HIE rat model, explore whether ferroptosis is involved in this pathological process, and evaluate the underlying mechanism *in vivo*.

## Materials and Methods

### Animals

A total of 100 healthy, male, specific pathogen-free (SPF) grade postnatal day 7 Sprague Dawley (SD) rats with an average weight of 12-17 g were purchased from Wuhan Cloud-Clone Animal Co., Ltd, Wuhan, China (Certificate No: SCXK (E) 2018-0021). All animals were housed in a steel cage at 22-25 °C with a 12 h light/dark cycle and ad libitum access to food and water throughout the study. The animal study was legally approved by the Animal Care & Welfare Committee of Wuhan Cloud-Clone Technology Co., Ltd.

### Establishment of the HIE model

As previously described, we used a modified Rice-Vannucci method to establish an HIE rat model [23]. Briefly, rats were anesthetized with isoflurane (induction concentration: 4 %, maintenance concentration: 2 %), the left common carotid artery was exposed and isolated from the vagus nerve, and double ligated with surgical silk. After the surgery, rats were placed in a 37 °C warming chamber for 60 min to recover. Subsequently, they were placed in a hypoxic chamber with 8 % oxygen balanced with nitrogen at 37 °C for 2 h. After hypoxia, the rats were returned to rest and placed in their home cage. The common carotid artery was isolated and exposed without ligation or hypoxia administration in the sham group rats.

### Animal grouping and drug administration

Farrerol was obtained from Shanghai Yuan Ye Bio-technology Co. Ltd. (Shanghai, China) and ML385 (Nrf2 specific inhibitor) from MedChemExpress (MCE). The rats were randomly allocated to five groups: sham group ( $n=20$ ), HIE group ( $n=20$ ), HIE + FA (40 mg/kg) group ( $n=20$ ), HIE + ML385 (30 mg/kg) group ( $n=20$ ),

and HIE + FA + ML385 group ( $n=20$ ). Except for the sham group, the HIE model was established according to the methods described above in all the other groups. Rats in the sham group were only isolated from the common carotid artery and without ligation or hypoxia administration. After modeling, the drug was administered intraperitoneally once a day for three consecutive days to the drug groups of rats. The same medium dose was intraperitoneally injected into the sham and HIE groups.

#### *Neurological severity score*

The neurological severity of rats was assessed using the Zea-Longa scoring system developed by Longa et al. [24] immediately after three days of intraperitoneal drug intervention. Specifically, the scores were: 0 points, no neurological deficit; 1 point, the tail was lifted and adduction (not able to fully extend) of the right forelimb was observed; 2 points, spontaneous circling to the right when walking; 3 points, the body was slanted to the right when walking; 4 points, not able to walk spontaneously along with possible loss of consciousness, with higher scores indicating more severe nerve injury. After neurological function assessment, animals in each group were sacrificed, and their whole brain tissues were harvested for subsequent experiments.

#### *Hematoxylin and eosin (HE) and Perls' Blue Staining*

For HE staining at day 10, the rats in all groups ( $n=5$ ) were deeply anesthetized, and their hearts were perfused with saline and 4% polyformaldehyde. The brain tissues were rapidly removed, fixed in 4% paraformaldehyde, dehydrated in gradient ethanol, embedded in paraffin, and cut into 4  $\mu\text{m}$ -thick coronal sections. The sections were then fixed, rinsed, and stained with hematoxylin and eosin (Solarbio Science & Technology, Beijing, China). For Perls' blue staining, the brain tissue sections were rinsed with phosphate-buffered saline (PBS) and stained with potassium ferrocyanide and nuclear fast red according to the manufacturer's instructions (Solarbio Science & Technology, Beijing, China). The morphologic changes and iron distribution were observed under a Leica microscope (DM4B, Germany) for five randomly selected areas.

#### *Fe<sup>2+</sup> ion content assay*

The rats in each group ( $n=5$ ) were deeply anesthetized and perfused with saline solution. The scalp and skull were cut, fresh brain tissues were harvested, and

the cerebral cortex tissue was separated for subsequent experiments. The Fe<sup>2+</sup> ion content in the cerebral cortex was determined using the iron assay kit (Abcam, ab83366) according to the manufacturer's instructions. Briefly, all groups of cerebral cortex samples (100 mg) were washed with cold PBS, homogenized with iron assay buffer on ice, the supernatant was collected, and the iron reducer was added. Consequently, the iron probe was added, mixed, and incubated for 1 h. The optical density was measured at 593 nm on a colorimetric microplate reader.

#### *Evaluation of infarct volume by 2,3,5-triphenyl-tetrazolium chloride (TTC) staining*

The TTC staining kit (Sigma-Aldrich, USA) was used to estimate the infarct volume [25]. The rats from each group ( $n=5$ ) were deeply anesthetized and perfused with saline solution. The fresh brain tissues were harvested and cut coronally into 2 mm thick sections. The sections were immersed in a 2% TTC solution and incubated at 37 °C for 30 min. The brain slices were frequently turned to ensure uniform staining, followed by PBS washing and photographing. The infarction region was stained white, while the remaining regions were stained red. The stained brain slices were placed on a scale, and images were captured. This volume was then divided by the total brain volume to obtain the percentage of brain infarction for subsequent statistical analysis with Image J. Infarct percentage = (infarct volume/the whole brain volume)  $\times$  100 %.

#### *Measurement of brain water content*

Rats from each group ( $n=5$ ) were sacrificed via decapitation and exsanguination. The cerebral hemispheres were separated, and the brain water content was determined using a weighing method. Fresh cerebral hemispheres tissues were harvested and weighed for the wet weight (WW). The tissues were then dried at 90 °C for 72 hours and weighed for the dry weight (DW). Based on the gravimetric differences, the brain water content was calculated as follows: Brain water content (%) = (WW-DW)/WW  $\times$  100 %.

#### *Reactive oxygen species (ROS) level assay*

To detect tissue ROS levels, 50 mg of fresh cerebral cortex tissue was accurately weighed and rinsed with PBS, followed by the addition of 1 mL of homogenate buffer A, according to the manufacturer's instructions (Biolab, Beijing, China). The tissue was fully

homogenized using a homogenizer and centrifuged at 10,000 g for 10 min at 4 °C. Subsequently, the supernatant was collected. 190 µl of the supernatant was taken and added with 10 µl probe. The mix was gently added to each well on a 96-well plate. The plate was incubated at 37 °C for 30 min in darkness, and the fluorescence intensity was detected using a fluorescent microplate reader (VICTOR Nivo, PerkinElmer, Lombard, USA) at an excitation wavelength of 485 nm and an emission wavelength of 610 nm. The ROS levels were expressed as a percentage of the control.

#### *Biochemical analysis*

Cerebral cortex tissues (100 mg) from all groups, as mentioned above, homogenate supernatant were acquired. The MDA, SOD, and GSH-Px levels in the supernatant were evaluated using commercial kits (Nanjing Jiancheng Bioengineering Institute, Nanjing, China) according to the manufacturer's instructions [26]. The MDA, SOD, and GSH-Px content were determined using thiobarbituric acid (TBA), WST-1, and colorimetric methods, respectively. The maximum absorbance of the compound was measured at 532, 550, and 412 nm, respectively, with a microplate reader (VICTOR Nivo, PerkinElmer, Lombard, USA).

#### *Western blotting*

A 200 mg sample of cerebral cortex tissue from each group was collected and homogenized in ice cold. As previously described, total protein and nuclear protein were isolated using RIPA lysis buffer or nuclear and cytoplasmic protein extraction kit (Beyotime, China) [27]. The protein concentration was determined using the bicinchoninic acid assay (BCA, Beyotime, China). The developed bands were visualized by enhanced chemiluminescence (ECL) advanced kit, and gel imaging was performed using ChemiDoc Touch (Bio-Rad).

## **Results**

#### *FA reduces neurological brain deficits, brain water content, and infarct volume in HIE rats*

The neurological deficits were evaluated using the Zea-Longa scoring system to explore the function of FA in this HIE model. The HIE group exhibited significantly higher scores of neurological deficits than the sham group, while treatment with FA or ML385 could significantly reduce or increase the neurological deficit scores compared with the HIE group, respectively.

However, combination treatment with ML385 and FA in HIE model rats increased the neurological deficit scores compared to the HIE + FA group (Fig. 1A). Furthermore, the TTC staining assay was performed to evaluate the cerebral infarct volume of different treatments in all groups. We found that the cerebral infarct volume in the HIE group was significantly increased. However, FA treatment in HIE model rats significantly reduced the infarct volume compared to the HIE group, while the opposite result was observed in the ML385 group. Combination treatment with ML385 and FA in HIE model rats significantly increased the cerebral infarct volume compared to the HIE + FA group (Fig. 1 B and 1C). Furthermore, the brain water content in all groups was evaluated. The results demonstrated that the brain water content in the HIE group was significantly increased compared to the sham group. However, treatment with FA or ML385 in HIE model rats significantly decreased or increased the brain water content compared to the HIE group, respectively. Combination treatment with ML385 and FA in HIE model rats significantly increased the brain water content compared to the HIE + FA group (Fig. 1D). These results indicate that FA has a protective function in HIE and can reduce neurological deficits, brain water content, and infarct volume. However, the combination treatment of ML385 and FA may have a negative effect on HIE.

#### *FA inhibits pathological brain injury and iron ion accumulation in HIE rats*

HE staining was performed to assess the structural and pathological changes in brain tissues of different treatment groups. In the sham group, the cell contour of cerebral cortex neurons was clear and normal, with distinct blue-stained nuclei in the center and cytoplasm without necrosis or degeneration. In the HIE group, neurons were lost, nuclei exhibited atrophy and pale pyknosis, and cytoplasm staining was uneven with damage. However, treatment with FA or ML385 ameliorated or deteriorated the pathological changes compared to the HIE group. Combination treatment with ML385 and FA in HIE model rats significantly deteriorated the pathological changes compared to the HIE + FA group (Fig. 2A). Furthermore, the iron ion accumulation in the cerebral cortex tissues was detected using Perls' staining, which is used to detect labile iron ion in biological tissues. The results showed that iron ion accumulation was significantly higher in the cerebral cortex of the HIE group compared to the sham group.

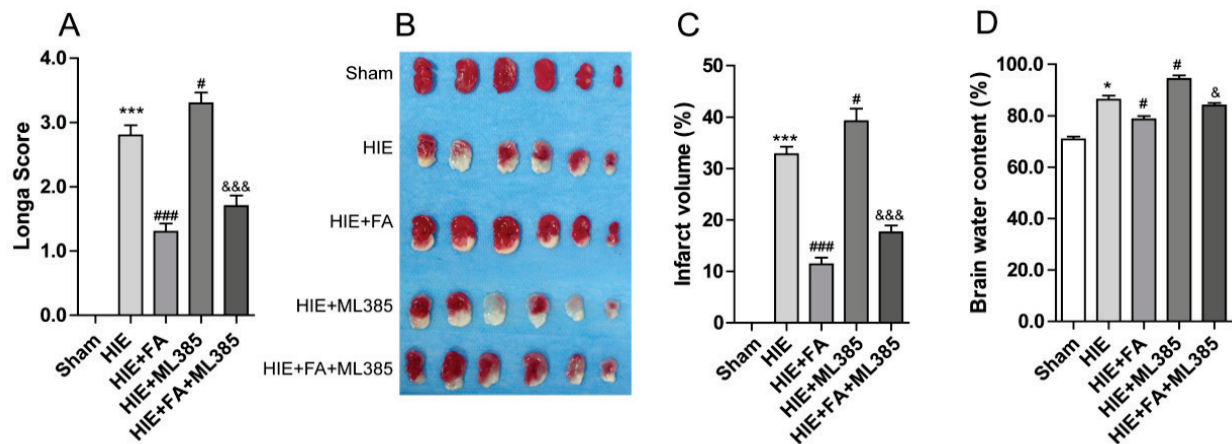


**Fig. 1.** FA attenuates HIE-induced neurological deficit scoring and cerebral infarction. **(A)** Zea-Longa scoring system was used to quantitative analysis the neurological behaviors of the rats. **(B)** TTC staining of representative images of coronal brain slices. White and red indicate infarct and normal tissues, respectively. **(C)** Quantitative evaluation of the brain infarct volume. **(D)** Quantitative analysis brain water content in all groups after HIE. Data were shown as the means  $\pm$  SEM, \* $p$ <0.05, \*\*\* $p$ <0.001 vs. the Sham group; # $p$ <0.05, ### $p$ <0.001 vs. the HIE group; & $p$ <0.05, && $p$ <0.001 vs. the HIE+FA group. HIE: Hypoxic-ischemic encephalopathy; SEM: standard error of the mean; TTC: 2,3,5-triphenyltetrazolium chloride.

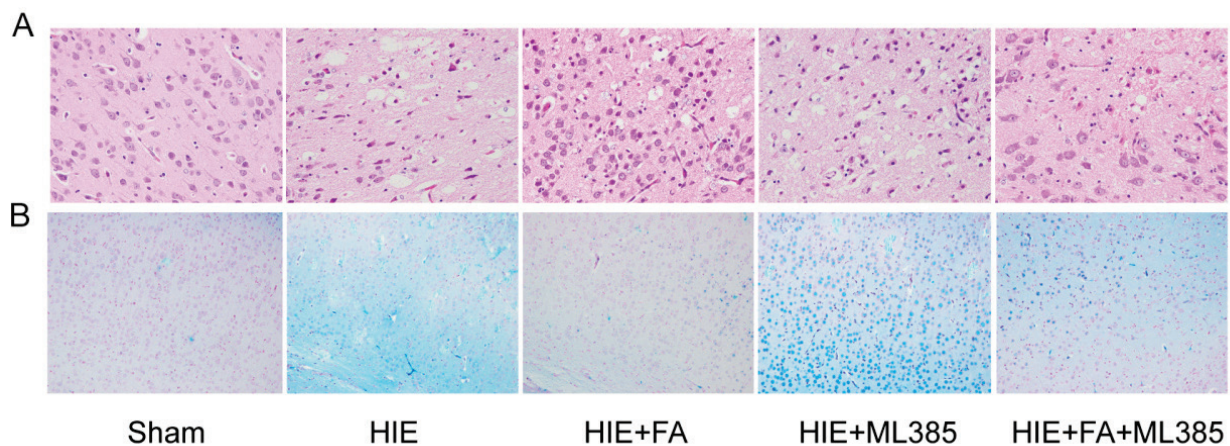


**Fig. 2.** FA alleviates pathological damage and iron ion deposit in HIE brain tissue. **(A)** The representative HE stained neuron cell morphology and structure in the brain tissue (400 $\times$ ). **(B)** Representative images of Perls' blue staining in different treatment group shown the iron ion accumulation (200 $\times$ ).

Treatment with FA or ML385 in HIE model rats reduced or increased iron ion accumulation compared to the HIE group in the cerebral cortex, respectively. Combination treatment with ML385 and FA in HIE model rats increased iron ion accumulation in the cerebral cortex compared to the HIE + FA group (Fig. 2B). These findings were supported by measuring the content of  $\text{Fe}^{2+}$  ions in the cerebral cortex (Fig. 3A). Overall, these results indicate that FA could protect neuron function, reduce iron ion accumulation, and alleviate pathological injury in HIE rats.

#### *FA alleviates hypoxic-ischemic-induced oxidative damage in HIE rats*

Oxidative damage is a major factor in HIE.

Spectrophotometer and colorimeter were used to evaluate the ROS, MDA, SOD, and GSH-Px levels in brain tissues of different treatment groups. The antioxidant indicators, both GSH-Px and SOD, were highly expressed in the sham group compared to the HIE group, while the oxidant indicator levels of ROS and MDA in the HIE group were significantly increased compared to the sham group (Fig. 3B-3E). Furthermore, treatment with FA or ML385 in HIE model rats increased or decreased the levels of GSH-Px and SOD, respectively, compared to the HIE group, while the levels of ROS and MDA showed opposite changes. Combination treatment with ML385 and FA in HIE model rats significantly decreased the expression of GSH-Px and SOD compared to the HIE + FA group. However, the MDA and ROS

expression levels in brain tissues showed opposite alteration compared to GSH-Px and SOD.

*FA inhibits hypoxic-ischemic-induced ferroptosis by activating the Nrf2 signaling pathway in HIE rats*

Nrf2 signaling pathways are important regulators implicated in ferroptosis. We explored the expression of related proteins using Western blot analysis. The results revealed that the ferroptosis inhibitor proteins, SLC7A11 and GPX4, were significantly decreased in the HIE group, while the expression proteins of Nrf2 in the nucleus and HO-1 were significantly increased in

response to stress compared to the sham group. However, FA treatment in HIE rats further elevated protein levels of Nrf2 in the nucleus and HO-1, and SLC7A11 and GPX4 were also enhanced compared to the HIE group, while ML385 treatment showed the opposite alteration. Furthermore, the combination treatment with ML385 and FA in HIE model rats further decreased the protein expression of SLC7A11, GPX4, Nrf2, and HO-1 compared to the HIE + FA group (Fig. 4A and 4F). Hence, these data suggested that FA could inhibit hypoxic-ischemic-induced ferroptosis by activating the Nrf2/HO-1 signaling pathway.

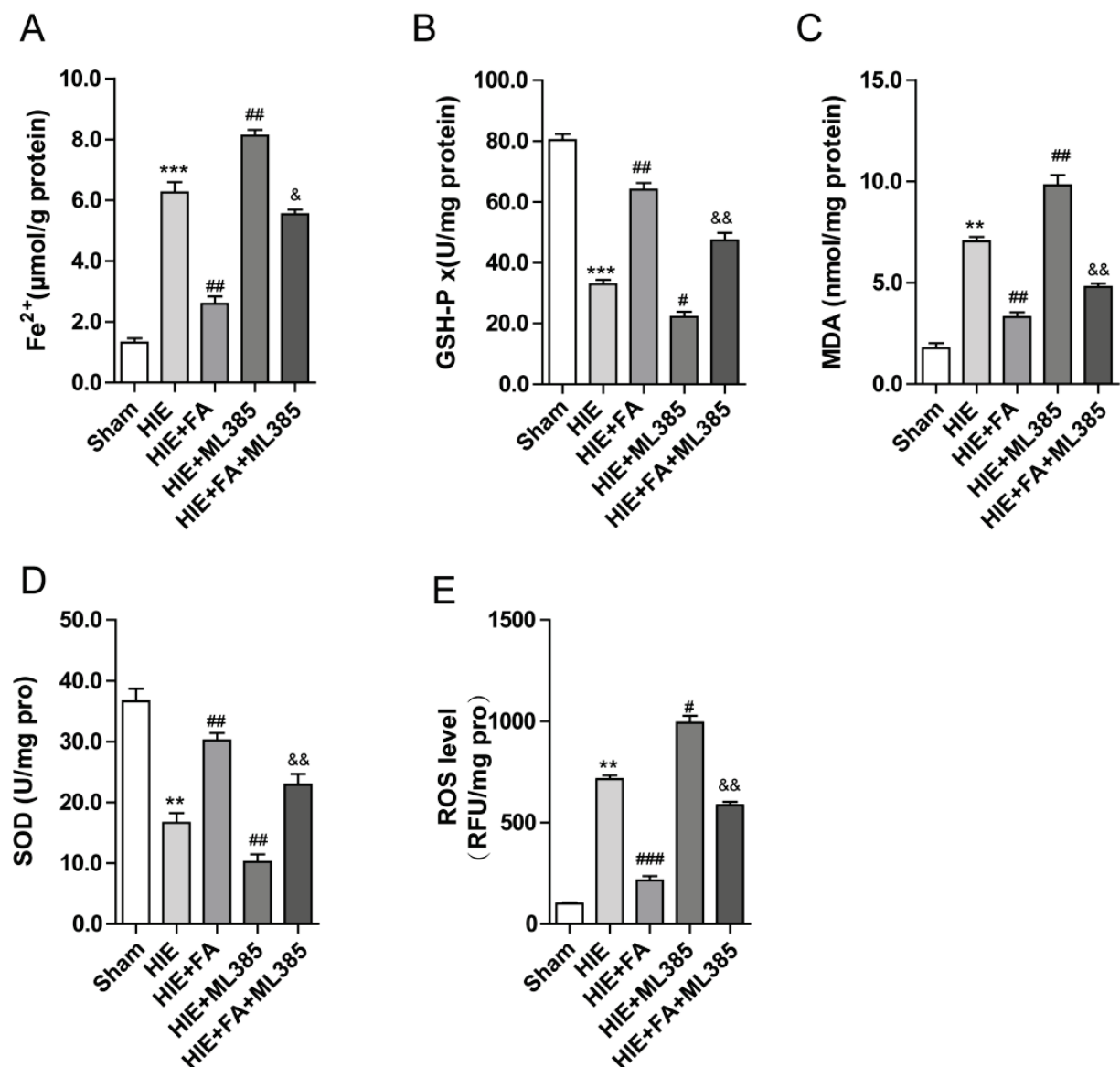


**Fig. 3.** FA alleviates oxidative stress parameters in HIE brain tissue. The level of Fe<sup>2+</sup> content (A), GSH-Px (B), SOD (C), MDA (D), and ROS (E) in cerebral cortex tissue were detected all groups and quantitative analysis. Data were presented as the mean ± SEM. \*\**p*<0.01, \*\*\**p*<0.001 vs. the Sham group; #*p*<0.05, ##*p*<0.01, ###*p*<0.001 vs. the HIE group; &*p*<0.05, &&*p*<0.01 vs. the HIE+FA group. HIE: Hypoxic-ischemic brain damage; SEM: standard error of the mean.



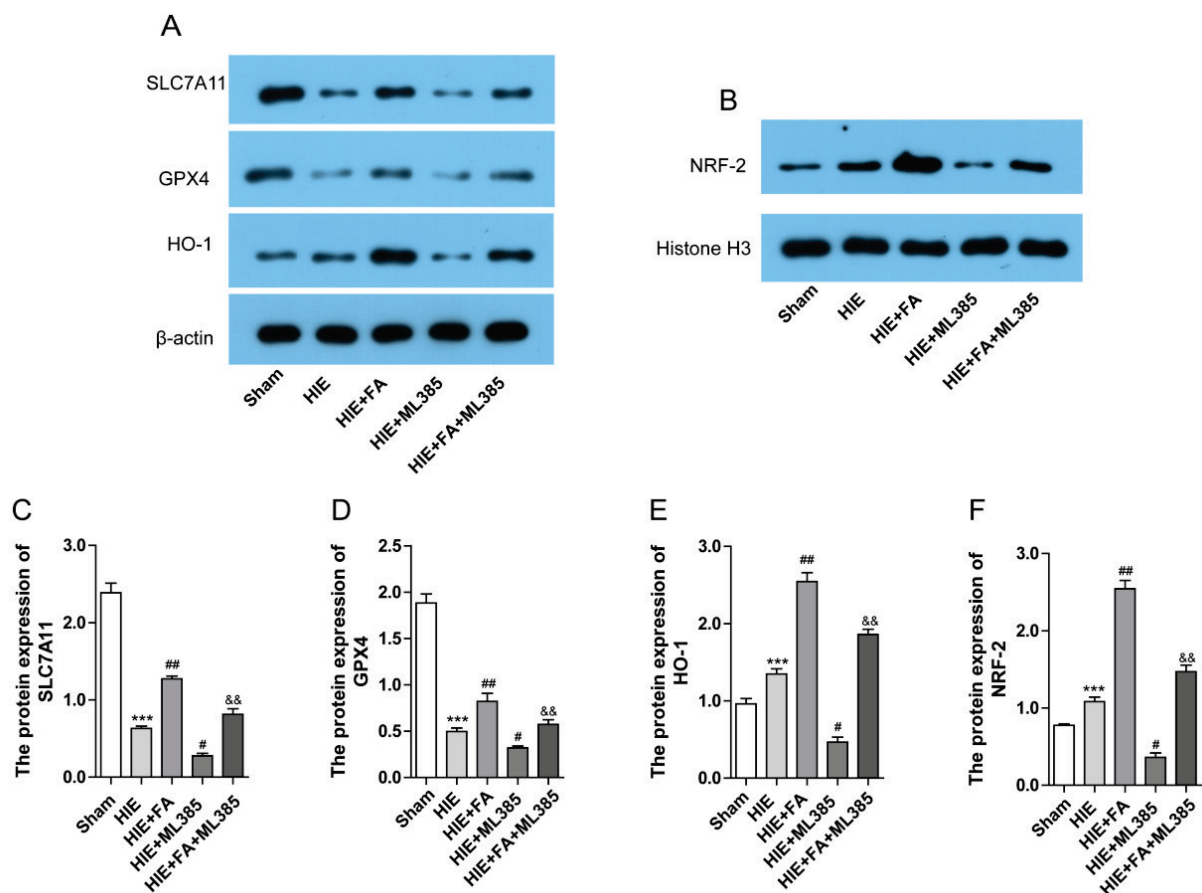


**Fig. 4.** FA alleviates HIE-induced ferroptosis by activating Nrf2 signaling pathway. **(A–B)** Representative western blotting of the protein expression levels of SLC7A11, GPX4, nuclear NFR-2 and HO-1 in cerebral cortex tissue. **(C–F)** Quantitative analysis of the protein expression of all groups. Data were presented as the mean  $\pm$  SEM. \*\*\* $p$ <0.001 vs. the Sham group; # $p$ <0.05, ## $p$ <0.01 vs. the HIE group; && $p$ <0.01 vs. the HIE+FA group. HIE: Hypoxic-ischemic encephalopathy; SEM: standard error of the mean.

## Discussion

In this study, we demonstrated the neuroprotective effect of FA in HIE rats. Cerebral infarction and brain edema are key indicators to evaluate the status of HIE. The degree of cerebral infarction and brain edema not only shows the acute brain injury but also reveals the neurological recovery ability. In this study, we demonstrated that FA could reduce cerebral infarct volume, brain water content, and iron ion accumulation in HIE rats, protecting neurons from damage, inhibiting the oxidative stress, increasing the expression of GSH-Px and SOD, and reducing the levels of MDA and ROS in brain tissues. Our findings also suggest that ferroptosis plays a role in promoting the progression of HIE. At the molecular level, FA's potential mechanism of action in protecting neurons from oxidative stress might be through activating the Nrf2 signaling pathway and promoting the upregulation of anti-ferroptosis markers SLC7A11 and GPX4.

FA is a traditional Chinese herbal medicine that has been reported to have a wide range of pharmacological effects, including anti-inflammatory, antioxidant, antitumor, and antimicrobial properties [16]. Oxidative stress participates in the pathogenesis of various diseases, including HIE. It disturbs the balance between the antioxidant defense system and results in excessive ROS production. Oxidative stress is considered the earliest pathological change after neonatal brain injury, making the brain vulnerable to oxidative damage. Several studies have found that oxidative stress could decrease the activity of several antioxidant enzymes, such as SOD and GSH-Px, which are critical factors involved in neuronal cell death in HIE [6, 28, 29]. SOD and GSH-Px are major antioxidant enzymes that protect cells from oxygen-free radical-induced injury and scavenge superoxide anions [30]. MDA is the end product of lipid peroxidation and a marker of oxidative stress. A previous study has demonstrated that FA is a novel Nrf2 activator that could improve cisplatin-induced nephrotoxicity by

activating Nrf2 [31]. In addition, a study has shown that FA protects against A $\beta$ -induced oxidative stress through the Nrf2/Keap1 pathway in microglia cells [20]. Similarly, FA treatment could markedly reduce the generation of intracellular ROS and MDA, increase the concentration of GSH and SOD, activate Nrf2, and increase the expression of HO-1 in retinal pigment epithelium cells [20]. Consistent with these reports, our study found that FA treatment of HIE rats increased the concentration of GSH-Px and SOD, reduced the level of MDA, ROS, and lipid peroxidation in brain tissue, and activated the Nrf2/HO-1 signaling pathway. Moreover, cerebral edema can lead to increased intracranial pressure, and brain edema can result in cellular swelling with fluid accumulating within the cell. We confirmed in the present study that experimental HIE elevated brain water content significantly, while FA treatment could significantly reduce it. Hence, our study further supports the view that FA treatment could exert antioxidant function in protecting neurons from oxidative damage.

The Nrf2/HO-1 signaling axis is a complex regulatory mechanism involved in oxidative stress diseases, exerting antioxidant effects in cellular oxidative stress processes [32]. In this study, we observed that the Nrf2/HO-1 signaling was activated in HIE, and FA treatment further enhanced this process. Additionally, the protective role of FA on the Nrf2/HO-1 signaling pathway was confirmed using a specific Nrf2 inhibitor (ML-385). Interestingly, the ferroptosis-relevant makers SLC7A11 and GPX4 were also found to be significantly down-regulated in HIE model rats, and FA treatment promoted the expression of these proteins. Previous studies have demonstrated that SLC7A11 and GPX4 are considered central regulators of ferroptosis, and changes in their levels are often involved in ferroptosis. The significant decrease in both SLC7A11 and GPX4 in HIE model rats suggests that ferroptosis occurred during the process of HIE. A recent study has revealed that FA could relieve collagenase-induced tendinopathy by inhibiting ferroptosis [33]. Therefore, our study provides further evidence that FA is involved in mediating ferroptosis. Furthermore, we noticed that ML-385 treatment not only reduced the expression of Nrf2 and HO-1 but also significantly reduced the expression of SLC7A11 and GPX4. These results suggest that the Nrf2/HO-1 signaling pathway regulates the expression of SLC7A11 and GPX4, which mediate ferroptosis in HIE.

These findings are consistent with previous reports indicating that activation of the Nrf2/HO-1 signaling pathway inhibits ferroptosis and increases the expression of ferroptosis-related proteins (SLC7A11 and GPX4) [34, 35]. Overall, our experimental results demonstrate that FA up-regulates the Nrf2/HO-1 signaling pathway and mediates ferroptosis, participating in the pathogenesis of HIE.

However, this study has some limitations, which must be overcome in future studies to further understand the function of FA in protecting neurons in HIE. Specifically, we only performed *in vivo* experiments; *in vitro* cell experiments are necessary to confirm our findings. Furthermore, diverse approaches, such as RNA interference and lentivirus transfection, should be employed to intervene in the expression of Nrf2 to confirm that FA targets Nrf2. Moreover, we observed that the expression of both Nrf2 and HO-1 was significantly increased in the HIE group compared to the sham group, even though the major function of Nrf2 signaling is to resist oxidative stress. Furthermore, while our current study revealed that FA treatment with HIE rats could alleviate ferroptosis by influencing the expression of hallmark SLC7A11 and GPX4, the expression of acyl-CoA synthetase long-chain family member 4 (ACSL4) as an essential component for ferroptosis execution was not detected. Moreover, the role of mitochondria in ferroptosis should be evaluated in all rat groups. Therefore, these limitations need to be addressed in subsequent research. Doing so may better demonstrate the role of FA treatment in HIE.

This study demonstrated that FA exerts protective effects against HIE in an *in vivo* model rat. Oxidative stresses, cerebral infarction, brain edema, iron ion accumulation, and neuron cell damage were alleviated in FA-treated rats subject to HIE damage. The underlying molecular mechanism might be that FA ameliorates oxidative stress in HIE via the Nrf2/HO-1/SLC7A11/GPX4 pathway. Overall, this study is the first to provide direct evidence for the potential of FA to exert neuroprotective effects by inhibiting neuron ferroptosis, making it a promising therapeutic agent in HIE.

### Conflict of Interest

There is no conflict of interest.



## References

1. Zhao M, Zhu P, Fujino M, Zhuang J, Guo H, Sheikh I, Zhao L and Li XK. Oxidative stress in hypoxic-ischemic encephalopathy: molecular mechanisms and therapeutic strategies. *Int J Mol Sci* 2016; 17. <https://doi.org/10.3390/ijms17122078>
2. Greco P, Nencini G, Piva I, Scioscia M, Volta CA, Spadaro S, Neri M, Bonaccorsi G, Greco F, Cocco I, Sorrentino F, D'Antonio F, Nappi L. Pathophysiology of hypoxic-ischemic encephalopathy: a review of the past and a view on the future. *Acta Neurol Belg* 2020; 120: 277-288. <https://doi.org/10.1007/s13760-020-01308-3>
3. Frajewicki A, Lastuvka Z, Borbelyova V, Khan S, Jandova K, Janisova K, Otahal J, Myslivecek J and Riljak V. Perinatal hypoxic-ischemic damage: review of the current treatment possibilities. *Physiol Res* 2020; 69: S379-S401. <https://doi.org/10.33549/physiolres.934595>
4. Yu S, Doycheva DM, Gamdzyk M, Gao Y, Guo Y, Travis ZD, Tang J, Chen WX, Zhang JH. BMS-470539 attenuates oxidative stress and neuronal apoptosis via MC1R/cAMP/PKA/Nurr1 signaling pathway in a neonatal hypoxic-ischemic rat model. *Oxid Med Cell Longev* 2022; 2022: 4054938. <https://doi.org/10.1155/2022/4054938>
5. Peeples ES and Genaro-Mattos TC. Ferroptosis: A Promising therapeutic target for neonatal hypoxic-ischemic brain injury. *Int J Mol Sci* 2022;23,7420: <https://doi.org/10.3390/ijms23137420>
6. Zhu K, Zhu X, Liu S, Yu J, Wu S, Hei M. Glycyrrhizin attenuates hypoxic-ischemic brain damage by inhibiting ferroptosis and neuroinflammation in neonatal rats via the HMGB1/GPX4 pathway. *Oxid Med Cell Longev* 2022; 2022: 8438528. <https://doi.org/10.1155/2022/8438528>
7. Lin W, Zhang T, Zheng J, Zhou Y, Lin Z, Fu X. Ferroptosis is involved in hypoxic-ischemic brain damage in neonatal rats. *Neuroscience* 2022; 487: 131-142. <https://doi.org/10.1016/j.neuroscience.2022.02.013>
8. Stockwell BR. Ferroptosis turns 10: Emerging mechanisms, physiological functions, and therapeutic applications. *Cell* 2022; 185: 2401-2421. <https://doi.org/10.1016/j.cell.2022.06.003>
9. Kuang G, Wang W, Xiong D Zeng C. An NADPH sensor that regulates cell ferroptosis. *J Transl Med* 2022; 20: 474. <https://doi.org/10.1186/s12967-022-03658-3>
10. Zeng C, Tang H, Chen H, Li M and Xiong D. Ferroptosis: a new approach for immunotherapy. *Cell Death Discov* 2020; 6: 122. <https://doi.org/10.1038/s41420-020-00355-2>
11. Zeng C, Lin J, Zhang K, Ou H, Shen K, Liu Q, Wei Z, Dong X, Zeng X, Zeng L, Wang W, Yao J. SHARPIN promotes cell proliferation of cholangiocarcinoma and inhibits ferroptosis via p53/SLC7A11/GPX4 signaling. *Cancer Sci* 2022;113:3766-3775. <https://doi.org/10.1111/cas.15531>
12. Wang X, Wang Y, Huang D, Shi S, Pei C, Wu Y, Shen Z, Wang F, Wang Z. Astragaloside IV regulates the ferroptosis signaling pathway via the Nrf2/SLC7A11/GPX4 axis to inhibit PM2.5-mediated lung injury in mice. *Int Immunopharmacol* 2022; 112: 109186. <https://doi.org/10.1016/j.intimp.2022.109186>
13. Li X, Chen J, Yuan S, Zhuang X, Qiao T. Activation of the P62-Keap1-NRF2 pathway protects against ferroptosis in radiation-induced lung injury. *Oxid Med Cell Longev* 2022; 2022: 8973509. <https://doi.org/10.1155/2022/8973509>
14. Chae J, Kim JS, Choi ST, Lee SG, Ojulari OV, Kang YJ, Kwon TK, Nam JO. Farrerol induces cancer cell death via erk activation in SKOV3 cells and attenuates TNF-alpha-mediated lipolysis. *Int J Mol Sci* 2021;22, 9400. <https://doi.org/10.3390/ijms22179400>
15. Yan C, Zhang X, Miao J, Yuan H, Liu E, Liang T, Li Q. Farrerol directly targets GSK-3beta to activate Nrf2-ARE pathway and protect EA.hy926 cells against oxidative stress-induced injuries. *Oxid Med Cell Longev* 2020; 2020:5967434. <https://doi.org/10.1155/2020/5967434>
16. Qin X, Xu X, Hou X, Liang R, Chen L, Hao Y, Gao A, Du X, Zhao L, Shi Y and Li Q. The pharmacological properties and corresponding mechanisms of farrerol: a comprehensive review. *Pharm Biol* 2022; 60: 9-16. <https://doi.org/10.1080/13880209.2021.2006723>
17. Ma N, Wei Z, Hu J, Gu W, Ci X. Farrerol ameliorated cisplatin-induced chronic kidney disease through mitophagy induction via Nrf2/PINK1 pathway. *Front Pharmacol* 2021; 12: 768700. <https://doi.org/10.3389/fphar.2021.768700>
18. Zhou L, Yang S, Zou X. Farrerol alleviates myocardial ischemia/reperfusion injury by targeting macrophages and NLRP3. *Front Pharmacol* 2022; 13: 879232. <https://doi.org/10.3389/fphar.2022.879232>

19. Wang L, Wei W, Xiao Q, Yang H, Ci X. Ferrerol ameliorates APAP-induced hepatotoxicity via activation of Nrf2 and autophagy. *Int J Biol Sci* 2019; 15: 788-799. <https://doi.org/10.7150/ijbs.30677>
20. Cui B, Zhang S, Wang Y and Guo Y. Ferrerol attenuates beta-amyloid-induced oxidative stress and inflammation through Nrf2/Keap1 pathway in a microglia cell line. *Biomed Pharmacother* 2019; 109: 112-119. <https://doi.org/10.1016/j.biopha.2018.10.053>
21. Li Y, Zeng Y, Meng T, Gao X, Huang B, He D, Ran X, Du J, Zhang Y, Fu S, Hu G. Ferrerol protects dopaminergic neurons in a rat model of lipopolysaccharide-induced Parkinson's disease by suppressing the activation of the AKT and NF-kappaB signaling pathways. *Int Immunopharmacol* 2019; 75: 105739. <https://doi.org/10.1016/j.intimp.2019.105739>
22. Cui B, Guo X, You Y, Fu R. Ferrerol attenuates MPP(+)-induced inflammatory response by TLR4 signaling in a microglia cell line. *Phytother Res* 2019; 33: 1134-1141. <https://doi.org/10.1002/ptr.6307>
23. Zhou Y, Wang S, Zhao J, Fang P. Asiaticoside attenuates neonatal hypoxic-ischemic brain damage through inhibiting TLR4/NF-kappaB/STAT3 pathway. *Ann Transl Med* 2020; 8: 641. <https://doi.org/10.21037/atm-20-3323>
24. Longa EZ, Weinstein PR, Carlson S, Cummins R. Reversible middle cerebral artery occlusion without craniectomy in rats. *Stroke* 1989; 20: 84-91. <https://doi.org/10.1161/01.STR.20.1.84>
25. Niu RZ, Xiong LL, Zhou HL, Xue LL, Xia QJ, Ma Z, Jin Y, Chen L, Jiang Y, Wang TH, Liu J. Scutellarin ameliorates neonatal hypoxic-ischemic encephalopathy associated with GAP43-dependent signaling pathway. *Chin Med* 2021; 16: 105. <https://doi.org/10.1186/s13020-021-00517-z>
26. Song S, Han Y, Zhang Y, Ma H, Zhang L, Huo J, Wang P, Liang M, Gao M. Protective role of citric acid against oxidative stress induced by heavy metals in *Caenorhabditis elegans*. *Environ Sci Pollut Res Int* 2019; 26: 36820-36831. <https://doi.org/10.1007/s11356-019-06853-w>
27. Zeng C, Shao Z, Wei Z, Yao J, Wang W, Yin L, YangOu H, Xiong D. The NOTCH-HES-1 axis is involved in promoting Th22 cell differentiation. *Cell Mol Biol Lett* 2021; 26: 7. <https://doi.org/10.1186/s11658-021-00249-w>
28. Zhu K, Zhu X, Sun S, Yang W, Liu S, Tang Z, Zhang R, Li J, Shen T, Hei M. Inhibition of TLR4 prevents hippocampal hypoxic-ischemic injury by regulating ferroptosis in neonatal rats. *Exp Neurol* 2021; 345: 113828. <https://doi.org/10.1016/j.expneurol.2021.113828>
29. Xiong Q, Li X, Xia L, Yao Z, Shi X, Dong Z. Dihydroartemisinin attenuates hypoxic-ischemic brain damage in neonatal rats by inhibiting oxidative stress. *Mol Brain* 2022; 15: 36. <https://doi.org/10.1186/s13041-022-00921->
30. Elias-Miro M, Jimenez-Castro MB, Rodes J, Peralta C. Current knowledge on oxidative stress in hepatic ischemia/reperfusion. *Free Radic Res* 2013; 47: 555-568. <https://doi.org/10.3109/10715762.2013.811721>
31. Ma N, Wei W, Fan X, Ci X. Ferrerol attenuates cisplatin-induced nephrotoxicity by inhibiting the reactive oxygen species-mediated oxidation, inflammation, and apoptotic signaling pathways. *Front Physiol* 2019; 10: 1419. <https://doi.org/10.3389/fphys.2019.01419>
32. Zhang X, Ding M, Zhu P, Huang H, Zhuang Q, Shen J, Cai Y, Zhao M, He Q. New insights into the Nrf-2/HO-1 signaling axis and its application in pediatric respiratory diseases. *Oxid Med Cell Longev* 2019; 2019: 3214196. <https://doi.org/10.1155/2019/3214196>
33. Wu Y, Qian J, Li K, Li W, Yin W, Jiang H. Ferrerol alleviates collagenase-induced tendinopathy by inhibiting ferroptosis in rats. *J Cell Mol Med* 2022; 26: 3483-3494. <https://doi.org/10.1111/jcmm.17388>
34. Ma H, Wang X, Zhang W, Li H, Zhao W, Sun J, Yang M. Melatonin suppresses ferroptosis induced by high glucose via activation of the Nrf2/HO-1 signaling pathway in type 2 diabetic osteoporosis. *Oxid Med Cell Longev* 2020; 2020: 9067610. <https://doi.org/10.1155/2020/9067610>
35. Fu C, Wu Y, Liu S, Luo C, Lu Y, Liu M, Wang L, Zhang Y, Liu X. Rehmannioside A improves cognitive impairment and alleviates ferroptosis via activating PI3K/AKT/Nrf2 and SLC7A11/GPX4 signaling pathway after ischemia. *J Ethnopharmacol* 2022; 289: 115021. <https://doi.org/10.1016/j.jep.2022.115021>